Substitution of Asparagine for Arginine 347 of Recombinant Factor Xa Markedly Reduces Factor Va Binding†

Amy E. Rudolph,* Rhonda Porche-Sorbet, and Joseph P. Miletich

Departments of Pathology and Medicine, Division of Laboratory Medicine, Washington University School of Medicine, St. Louis, Missouri 63110

Received October 13, 1999; Revised Manuscript Received December 14, 1999

ABSTRACT: Herein we describe a recombinant factor X (fX) with a single substitution at position 347 (fX**R347N**). Activated fX**R347N** had a reduced affinity for factor Va (fVa), although the catalytic impact of fVa binding remained intact. The mutation was selective as demonstrated by normal activation and inhibition, except in the presence of subsaturating heparin where the rate of inhibition by antithrombin III (ATIII) was 15% of normal. The reactivity of fXa**R347N** toward prothrombin was equivalent to wild-type fXa (fXa**WT**) in the absence of fVa and phospholipid. Addition (without phospholipid) of fVa dramatically increased the catalytic efficiency of fXa**WT** toward prothrombin but had a negligible effect on fXa**R347N**. On addition of phosphatidylcholine:phosphatidylserine (PC:PS, 3:1) vesicles, fXa**R347N** displayed an increased catalytic activity in response to fVa, but the apparent affinity for fVa on the phospholipid surface was 5−20-fold lower than that of fXa**WT**. On an activated platelet surface, however, fXa**WT** and fXa**R347N** activated prothrombin similarly. In a competitive binding assay that measures the displacement of radiolabeled fXa from fVa on a phospholipid surface, fXa**R347N** was ∼10-fold less effective than fXa**WT**. Substitution of fXa at position 347 selectively attenuates the interaction between fXa and fVa without affecting its catalytic activity.

The vitamin K-dependent plasma serine protease fXa holds a pivotal position in blood coagulation as the only known physiological activator of prothrombin. The zymogen precursor, fX, is activated to fXa in the presence of calcium by complexes in the intrinsic (fIXa/fVIIIa) and extrinsic (fVIIa/TF)[1] pathways and by RVV-X (*1*−*6*). Activated fX is inhibited by antithrombin III (ATIII) and tissue factor pathway inhibitor [TFPI (*7*−*10*)]. The light chain of fX contains 11 γ-carboxylated glutamic acid residues in the amino terminal gla domain, which are necessary for the membrane binding capacity of the molecule, followed by two epidermal growth factor-like domains (EGF1 and EGF2). The heavy chain, which contains the activation peptide and the serine protease domain, is joined to the light chain by a single disulfide bond.

As the enzymatic component of the prothrombinase complex, fXa interacts with the surface (membrane phospholipid), the cofactor (fVa), and the substrate (prothrombin) for maximally efficient thrombin formation (*11*). Determining the contribution of specific intermolecular interactions within the prothrombinase complex to the overall catalytic activity of fXa is therefore complex. Ideally, each interaction should be characterized independently and combinatorially.

Although the methodology for expression of recombinant fX has been developed (*12*, *13*), it only affords the production of limited quantities. This precludes direct analysis of the binding between recombinant fXa and other components of the prothrombinase complex by conventional means. However, these interactions can be assessed by examining the influence of the components on fXa catalytic function. In addition, we describe a novel competitive binding assay which measures the interaction between fXa and fVa on a phospholipid surface in the absence of prothrombin. Using these techniques, we have characterized a recombinant variant fX species that has a single substitution at position 347 (residue 165 in chymotrypsin numbering). This variant fXa (fXa**R347N**) demonstrates a selective reduction in the fVa affinity of fXa.

MATERIALS AND METHODS

Materials. Crude snake venoms, L-α-phosphatidylcholine, and L-α-phosphatidylserine were purchased from Sigma. Spectrozyme TH (H-D-hexahydrotyrosyl-L-alanyl-L-arginine-*p*-nitroanalide-diacetate) and Spectrozyme FXa (methoxycarbonyl-D-cyclohexylglycyl-glycyl-arginine-*p*-nitro-anilide-acetate) were purchased from American Diagnostica Inc. (Greenwich, CT). Full-length heparin was obtained from Elkins-Sinn Inc. (Cherry Hill, NJ). Heparin pentasaccharide was a generous gift of J. C. Lormeau of Sanofi Recherché (Gentilly Cedex, France). All other reagents and chemicals were of the highest quality available commercially.

Proteins. Prothrombin was purified, concentrated (to >1 mM), and immunodepleted of residual fX (<1 nM) as

† This work was supported in part by grants from the National Institutes of Health (NHLBI HL14147) and the Monsanto/Searle Company.

* To whom correspondence should be addressed. Present address: Monsanto/Searle, 800 North Lindbergh Boulevard, St. Louis, MO 63167. Phone: (314) 694-9017. Fax: (314) 694-8153. E-mail: amy.e.rudolph@monsanto.com.

[1] Abbreviations: TF, human tissue factor; Hepes, (*N*-[2-hydroxyethyl]piperazine-*N*′-[2-ethanesulfonic acid]); PEG, poly(ethylene glycol) 8000; BSA, bovine serum albumin; EDTA, ethylenediaminetetraacetic acid; SDS−PAGE, sodium dodecyl sulfate−polyacrylamide gel electrophoresis; RVV-X, X activating protein from Russell's viper venom.

10.1021/bi992379b CCC: $19.00
Published on Web 02/23/2000

described (*12*). Factor VII was purified from human plasma (*14*). Antithrombin III was purchased from Kabi Pharmacia Diagnostics (Piscataway, NJ) and recombinant TFPI was a gift of Monsanto/Searle Company (St. Louis, MO). Human fVa and fIXa were purchased from Haematologic Technologies (Essex Jct., VT). Thrombin was prepared by cation-exchange chromatography after activation of human prothrombin with Taipan snake (Oxyuranus scutellatus) venom. Porcine fVIII was obtained from Porton Products (Agoura Hill, CA) and was further purified (*15*) using an immobilized antibody (W-3, a generous gift from Dr. David Fass). Innovin, a lipidated, recombinant tissue factor, was obtained from Baxter Diagnostics (Deerfield, IL). RVV-X was purified from Russell's viper venom (*16*). SDS−PAGE was performed by the method of Laemmli (*17*). Proteins were stained directly using Coomassie Blue or were transferred to nitrocellulose (0.45 nm), probed using antibodies described previously (*12*), and visualized with an immunochemiluminescent kit (Amersham, Buckinghamshire, U.K.). The secondary antibody utilized for immunoblotting was affinity-purified caprine anti-mouse IgG conjugated to horseradish peroxidase, Jackson ImmunoResearch (West Grove, PA).

FX was purified from culture media as previously described (*12*, *13*). Briefly, fX was removed from media by absorption to barium citrate. The resulting pellet was washed and resuspended in 32% saturated NH_4SO_4 in the presence of 5 mM diisopropylfluorophosphate and incubated for 1 h at 4 °C. The precipitate was collected by centrifugation and the resulting supernatant was dialyzed into 1 mM benzamidine, 10 mM Hepes, and 100 mM NaCl, pH 7.0. The dialyzed supernatant was concentrated, clarified by centrifugation at 12000*g*, and immunoaffinity purified using antibody 3698.1A8.10, a calcium-dependent monoclonal antibody directed against the Gla domain of fX. Separate columns were used for fX**WT** and fX**R347N**. FX was eluted with 5 mM EDTA, 10 mM Hepes, and 100 mM NaCl, pH 7.0, and pooled fractions containing fX were loaded onto a Pharmacia Mono Q FPLC column. FX was eluted with a high-salt buffer (10 mM Hepes and 500 mM NaCl, pH 7.0). Fractions containing fX antigen were pooled and adjusted to pH 6.5 and final concentrations of 2.5 mM $CaCl_2$ and 20% glycerol for storage at −70 °C.

Defined Phospholipid Vesicles. PC:PS (3:1) vesicles, of nominal 100 nm diameter, were synthesized from egg yolk phosphatidylcholine (PC) and bovine brain phosphatidylserine (PS) at a concentration of 1.0 mM total lipid in 5 mM $CaCl_2$, 10 mM Hepes, and 100 mM NaCl, pH 7.5, by the method of membrane extrusion (*18*) using the Liposofast Basic device (Avestin, Ottawa, ON, Canada). Vesicles were adjusted to a final concentration of 10% (v/v) glycerol, snap frozen, and stored at −70 °C.

Purity and Concentration. The overall quality of the purified fX species was determined by SDS−PAGE. The total protein concentration was determined using the reported (*2*) extinction coefficient for plasma fX ($OD_{280\ nm,E}^{mg/mL} = 1.16$) and agreed with the fX concentration determined by a two-site immunoassay (*12*). Activation of recombinant fX was also monitored by following the loss of signal over time in an immunoassay using monoclonal antibodies directed against the activation peptide and the light chain (3514.2E12.1 and 3448.1D7.20, respectively, *12*).

Construction and Cell Culture. The recombinant fX constructs were made as described (*12*, *13*). All mutations were introduced using a Transformer mutagenesis kit (Clonetech, Palo Alto, CA). Mutations were engineered into the cDNA of fX, which had been cloned from a human hepatocyte library and inserted into pUC19. Arg347 was mutated to alanine to evaluate the contribution of this residue to fXa function. To create a reagent for a competition binding assay which requires a fXa molecule with equivalent binding capacity to wild-type fXa, but lacking the capacity for autolysis (see below), a second mutant was made in which the active-site serine was substituted by alanine. Substitutions introduced at Arg347 and Ser379 generated new *Hin*cII and *Xcm*I restriction sites, respectively, which were used to evaluate mutant clones for successful mutagenesis. The mutations, as well as the entire wild-type sequence, were verified by sequencing. Constructs were shuttled into a mammalian expression vector (ZMB3), which was kindly provided by Dr. Don Foster (ZymoGenetics). Human kidney cells (293 cells, ATCC-CRL-1573) were transfected using calcium phosphate precipitation (*19*) and cultured as previously described (*12*, *13*). The fX produced was screened for concentration, size, and function by immunoassay, by immunoblotting after SDS−PAGE and by a modified prothrombin time assay, respectively. Selected clones were expanded for media conditioning.

Activation. Activation of 100 nM fX**R347N** by (1) 50 pM RVV-X (to determine the initial rate) or 2 nM RVV-X (to determine the extent), (2) 40 pM fVIIa in the presence of 0.5 nM lipidated tissue factor, and (3) 2 nM fIXa in the presence of 4 units/mL fVIIIa on 20 μM PC:PS vesicles was directly compared to activation of 100 nM fX**WT**. To determine fXa concentrations, aliquots of the reactions were removed over time, quenched into an EDTA-containing buffer, and incubated with 100 μM Spectrozyme FXa. Initial rates of Spectrozyme FXa hydrolysis were determined with a Molecular Dynamics (Sunnyvale, CA) kinetic microplate reader and fXa concentrations were calculated by reference to standard curves constructed from dilutions of completely activated fXa**WT** or fXa**R347N**.

Inhibition Studies. Inhibition of the variant and wild-type enzyme was evaluated using standard methods (*12*, *13*, *20*−*21*). Both zymogens (100 nM in assay buffer) were activated to completion by RVV-X (2 nM), as monitored by activity and by SDS−PAGE analysis. The enzymes were diluted to 0.5 nM in assay buffer and incubated with 100 μM Spectrozyme FXa in the presence of various concentrations of inhibitors: (1) 0−4 μM ATIII, (2) 0−50 nM ATIII in the presence of 0.5 μM heparin pentasaccharide, (3) 0−16 nM ATIII in the presence of a subsaturating concentration (2.5 munits/mL) of heparin, or (4) TFPI (0−50 nM). The appearance of the chromophore, *p*-nitroanilide acetate (pNA), was monitored over time at 405 nm. Primary data were fitted, using the Marquardt-Levy algorithm (SigmaPlot, Jandel Scientific, Corte Madera, CA), to an exponential equation of the form

$$A = A_f(1 - e^{-k_{obs}t}) + A_o$$

where A is the observed absorbance, A_f is the amplitude of the curve, k_{obs} is the apparent first-order rate constant (s^{-1}), t is time in seconds, and A_o is the initial absorbance. Each

calculated apparent rate constant (k_{obs}) was then plotted as a linear function of the effective inhibitor concentration, and the resulting slope was calculated as the apparent second-order rate constant.

Thrombin Formation. In all cases, the variant fX species was compared to recombinant wild-type. Kinetic values were derived from the least-squares fit of the data based on the equation

$$v = V_{max}[Z]/(K_{app} + [Z])$$

where v is the observed initial rate of thrombin formation, V_{max} is the maximal initial rate of thrombin formation, [Z] is the concentration of the component being varied in the experiment, and K_{app} is the apparent concentration of the variable component required to reach half-maximal thrombin formation under the conditions specified.

Thrombin generation by 10 nM fXa from prothrombin alone was characterized by varying the prothrombin concentration (0−1 mM). Thrombin formation from 10 μM prothrombin by 0.5 nM fXa in the presence of fVa was quantitated over a range of fVa concentrations (0−1.0 μM). Thrombin generation on 20 μM PC:PS vesicles was determined using 20 pM fXa, 1.0 μM prothrombin, and varying fVa from 0 to 1.0 nM. Thrombin formation from 1.0 μM prothrombin on 10^8/mL thrombin activated (0.5 units/mL) platelets was tested over a range of fXa concentrations (0−1.0 nM). In all experiments, aliquots were removed from the reaction tube at specified times and diluted at least 10-fold into EDTA buffer (5 mM EDTA, 1 mg/mL PEG 8000, 1 mg/mL BSA, 10 mM Hepes, 100 mM NaCl, pH 7.4). A saturating concentration (500 μM) of the thrombin chromogenic substrate, Spectrozyme TH, was added to quenched samples and the appearance of the chromophore, *p*-nitroanilide acetate (pNA), was monitored over time at 405 nm. The concentration of thrombin formed was calculated by comparison to a standard curve using purified thrombin. The assay buffer used in all experiments, unless otherwise noted, was 5 mM $CaCl_2$, 1 mg/mL PEG 8000, 1 mg/mL BSA, 10 mM HEPES, 100 mM NaCl, pH 7.4.

Competition Binding Assay. FX**S379A** was labeled with ^{125}I using Bolton−Hunter reagent, Amersham (Arlington Heights, IL), in a modified procedure. After the supplied solvent was evaporated under nitrogen, fX**S379A**, pH 8.5, was added and incubated for 1 h on ice. Hepes (10 mM), 100 mM NaCl, and 200 mM glycine, pH 7.4, were added for an additional 5 min on ice. Radioactivity not incorporated into protein was removed using a Bio-Spin 6 column, Bio-Rad Laboratories (Hercules, CA). The specific activity of the labeled protein was typically 2000 cpm/ng. Labeled FX**S379A** was activated using RVV-X as described above and stored at −70 °C in 20% glycerol (v/v).

A latex bead-based binding assay was developed based on published methods (*22*). Carboxyl latex beads (1.0 μm) from Interfacial Dynamics Corp. (Portland, OR) were washed exhaustively in 1% ethanol, followed by water, and then lyophilized. The dried beads (20 mg) were mixed with 3.8 μmol of PC:PS (3:1) in hexane:ethanol (9:1) to provide a ratio of lipid surface area to bead surface area of ∼10. The suspension was sonicated and then dried under nitrogen. The dried bead pellet was washed in assay buffer and the beads were collected by centrifugation at 12000*g* and resuspended in 1.0 mL of assay buffer. Beads coated with PC only were also prepared and used in pilot experiments to demonstrate specificity, i.e., no fVa-dependent binding without PS. Nonspecific binding accounted for <10% of binding, and approximately 50% of [^{125}I]fXa**S379A** binding was prevented by the addition of 1 nM unlabeled fXa**WT**.

The concentrations of all assay components were empirically determined. PC:PS-coated beads were added at a final concentration of 0.2% (v/v). This concentration of beads was determined to be equivalent to 20 μM PC:PS vesicles for supporting thrombin formation by fXa**WT** in the presence of fVa. Uncoated beads prepared in the same manner but with no lipid added were added at a final concentration of 0.8% (v/v) to aid centrifugation and pellet visualization; uncoated beads were otherwise without effect in the assay. The amount of fVa required to support approximately 80% of the maximal thrombin generation rate with 1 μM prothrombin and saturating fXa**WT** was established at 1 nM. The amount of [^{125}I]fXa**S379A** needed to reach approximately 80% of maximal specific binding at this concentration of fVa was determined to be 1 nM. In the assay, 1 nM fVa was incubated with 0.2% (v/v) PC:PS beads and 0.8% (v/v) uncoated beads for 10 min. [^{125}I]fXa**S379A** (final concentration 1.0 nM) was mixed with increasing concentrations of either fXa**WT** (0−7.0 nM) or fXa**R347N** (0−50 nM), added to the fVa/bead mixture, and incubated with mixing for an additional 10 min. [^{125}I]fXa**S379A** was utilized as the labeled fXa species for greater stability over time, i.e., to minimize fXa-dependent proteolysis. The beads were collected by centrifugation, and the pellets and supernatants were counted separately. Nonspecific binding was determined from reactions not containing fVa and subtracted from all counts bound in the pellets. The percentage of specific bound fXa was quantitated based on reactions with no unlabeled fXa.

Structure. The structure of fXa was visualized from the published coordinates (*23*) using RasMol v2.5, developed by Roger Sayle at Glaxo Research and Development (Greenford, Middlesex, U.K.). In the structure, the Gla domain is missing, EGF1 is disordered, and residues 329−333 are disordered or missing, so these regions are not visualized.

RESULTS

Mutational Methodology. The expression system affords production of fully functional wild-type fX and variant fX species that have been selectively mutated (*12*, *13*). The variant fX used in this study differed from wild-type only in that residue 347 was changed to asparagine (PYVD**R**NSCK → PYVD**N**NSCK), thereby eliminating the charge on this surface residue. We considered the possibility that this mutation also created a new N-linked glycosylation site. However, as indicated by the equivalent electrophoretic mobility of fX**R347N** and fX**WT** (Figure 1), Asn347 in the mutant was not glycosylated.

Activation. The affinity and maximal turnover rate of Spectrozyme FXa were very similar for fXa**WT** and fXa**R347N** (K_m = 70 versus 75 μM; V_{max} = 45 versus 39 μM pNA/min, respectively). Therefore, this substrate was used to monitor initial rates and extents of activation as described in the Materials and Methods. Activation of fX**R347N** by RVV-X, the intrinsic Xase complex (fIXa/fVIIIa), and the extrinsic Xase complex (fVIIa/TF) was equivalent to those of fX**WT** (data not shown).

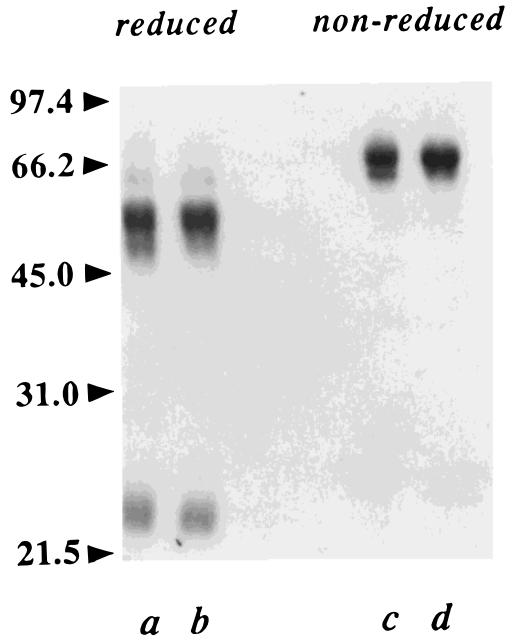

FIGURE 1: SDS−PAGE of WT and variant fX species. Proteins were analyzed using a 12.5% separating gel. The gel was stained with Coomassie Blue. Each lane contains 1.5 μg of protein. Lane a is reduced fX**WT**. Lane b is reduced fX**R347N**. Lane c is nonreduced fX**WT**. Lane d is nonreduced fX**R347N**.

Table 1: Inhibition of fXa**R347N** and fXa**WT**

inhibitor	second-order rate constants [M^{-1} s^{-1} × 10^4 (mean ± SE)] fXa**WT**	fXa**R347N**
TFPI[a]	11.3 ± 1.6	10.7 ± 0.6
ATIII[a]	0.16 ± 0.02	0.14 ± 0.03
ATIII + PS[b]	21.1 ± 1.8	17.1 ± 2.5
ATIII + HEPARIN[c]	155.4 ± 0.3	23.4 ± 0.7

[a] fXa (0.5 nM) was incubated with varying concentrations of recombinant TFPI (0−50 nM) or ATIII (0−4 μM). [b] fXa (0.5 nM) was incubated with varying concentrations of ATIII (0−50 nM) in the presence of 0.5 μM heparin pentasaccharide. [c] fXa (0.5 nM) was incubated with varying concentrations of ATIII (0−16 nM) in the presence of full-length heparin (2.5 munits/mL). Second-order rate constants were determined as described in the Materials and Methods.

Inhibition. Inhibition of activated fX**R347N** by TFPI and ATIII was compared directly to inhibition of fXa**WT** (Table 1). TFPI and ATIII inhibited the fXa**R347N** and fXa**WT** at the same rate. ATIII in the presence of a heparin pentasaccharide also inhibited fXa**R347N** at a normal rate. In the presence of a subsaturating concentration of full-length heparin, however, fXa**R347N** was only inhibited at 15% of the normal rate. The second-order rate constants for inhibition by ATIII in the presence of this concentration of heparin were 155.4 × 10^4 versus 23.4 × 10^4 M^{-1} s^{-1} for fXa**WT** and fXa**R347N**, respectively. The values for fXa**WT** are similar to reported values (*24*).

Prothrombin Activation in the Absence of a Phospholipid Surface. To evaluate the function of fXa**R347N** relative to fXa**WT**, the initial rates of prothrombin activation by each enzyme were determined at different prothrombin concentrations (see Materials and Methods). The activity of fXa**R347N** toward prothrombin in the absence of fVa and phospholipid was equivalent to that of fXa**WT** (Figure 2); measured K_m values for prothrombin were 188 and 155 μM, while turnover

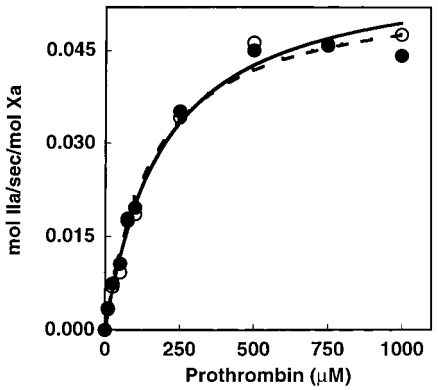

FIGURE 2: Generation of thrombin by fXaWT and fXaR347N in the absence of phospholipid and fVa. fXa**WT** (10 nM) (●) or fXa**R347N** (○) was incubated with varying concentrations of prothrombin (0−1 mM). Aliquots were removed from the reactions over time (0−10 min), diluted 10-fold into EDTA-containing buffer, and incubated with 0.5 mM Spectrozyme TH. The initial rate of hydrolysis was monitored at 405 nm. The concentration of thrombin was determined from a standard curve prepared from dilutions of maximally activated prothrombin. The rate of thrombin formation at each prothrombin concentration was then calculated and expressed as moles of thrombin (IIa) per second per mole of Xa.

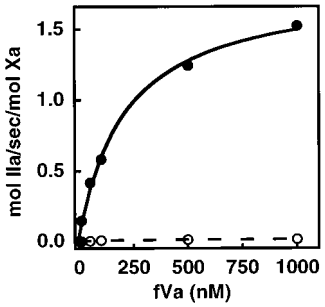

FIGURE 3: Thrombin generation by WT and variant fXa in the absence of phospholipid and in the presence of fVa. fXa**WT** (0.5 nM) (●) or fXa**R347N** (○) was incubated with 10 μM prothrombin and varying concentrations of fVa (0−1 μM). Aliquots were removed from each reaction over time (0−8 min) and the initial rate of thrombin formation was determined at the fVa concentrations indicated as described in the legend to Figure 2.

rates were 0.059 and 0.055 mol of thrombin/s/mol of fXa for fXa**R347N** and fXa**WT**, respectively.

The catalytic activity of fXa**WT** toward prothrombin is markedly enhanced by fVa, e.g., at 10 μM prothrombin, fXa**WT** was catalytically more than 1000 times faster in the presence of 500 nM fVa. In contrast, the activity of fXa**R347N** was not detectably affected at fVa concentrations as high as 1 μM (Figure 3). Since fXa**R347N** interacts with and cleaves prothrombin normally in the absence of fVa (Figure 2), it either has a much weaker affinity for fVa or fVa/prothrombin relative to fXa**WT** or it cannot undergo structural rearrangements induced by fVa that increase the catalytic activity (*25*−*26*).

Prothrombin Activation in the Presence of Phospholipid. It has been suggested that appropriate phospholipid surfaces increase the local concentrations of fXa and fVa, thus maximizing complex formation (*27*−*30*). Defined phospholipid surfaces such as PC:PS (3:1) vesicles can support thrombin generation by fXa and fVa. Although limiting quantities of human fVa precluded quantitation of the maximal prothrombin turnover under these conditions, the apparent affinity of fXa**R347N** was at least 5-fold lower than that of fXa**WT** for fVa on the vesicles (Figure 4).

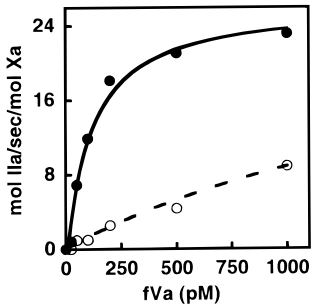

FIGURE 4: Thrombin generation on PC:PS vesicles in the presence of cofactor. fXa**WT** (20 pM) (●) or fXa**R347N** (○) was incubated with 20 μM PC:PS vesicles, 1 μM prothrombin, and varying concentrations of fVa (0−1 nM). Aliquots of each reaction were removed over time (0−3 min) and quenched into EDTA-containing buffer. Initial rates of thrombin formation were determined for each fVa concentration as described in the legend to Figure 2.

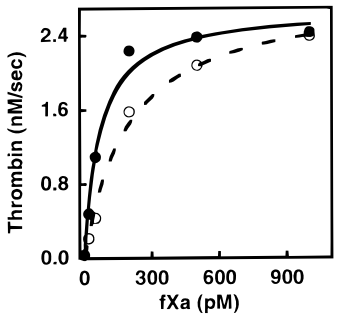

FIGURE 5: Generation of thrombin by fXa**WT** and fXa**R347N** on an activated platelet surface. Washed platelets were incubated at 10^8/mL with 0.5 units/mL thrombin and fXa at varying concentrations (0−1 nM). The reaction was initiated by addition of 1.0 μM prothrombin. Thrombin generation was quantitated for fXa**WT** (●) or fXa**R347N** (○) by quenching aliquots of each reaction over time (0−3 min) into EDTA-containing buffer. Each aliquot was subsequently incubated with 0.5 mM Spectrozyme TH and the initial rate of thrombin formation was quantitated from Spectrozyme TH hydrolysis as described in the legend to Figure 2.

Since activated platelets provide both the best known surface for prothrombinase complex assembly and saturating amounts of fVa, the generation of thrombin on platelets (10^8/mL) was examined. Under these conditions, fXa**WT** and fXa**R347N** showed similar activity with apparent affinities for the platelet surface of 134 and 186 pM and maximal rates of thrombin formation of 2726 and 2907 pM s^{-1}, respectively (Figure 5).

Competition Binding Assay. On the basis of these observations, the simplest explanation for the phenotype of fXa**R347N** is a selective attenuation of the interaction with fVa. However, since the functional studies rely on the amplification inherent in generating thrombin from prothrombin, it is possible that the reduced affinity is for a fVa/prothrombin complex rather than for fVa alone. The relatively low affinity of fXa for fVa in the absence of all other prothrombinase complex components [~1 μM (*31*, *32*)] precluded direct examination of the binary interaction by conventional methods with the limited available quantities of the recombinant proteins and fVa. A competition binding assay was, therefore, developed to examine the interaction between fVa and the fXa species on a phospholipid surface in the absence of prothrombin.

The assay employed PC:PS-coated latex beads and radiolabeled factor Xa containing an alanine substitution at the active-site serine ([^{125}I]fXa**S379A**). In the binding studies, the fVa was preincubated with the coated beads. Then, increasing concentrations of fXa**WT** or fXa**R347N** mixed with the fixed amount of ^{125}I-labeled fXa**S379A** were allowed to compete for the bound fVa. As shown in Figure 6, fXa**R347N** was ~10-fold less potent than fXa**WT** in competing with [^{125}I]fXa**S379A** for fVa binding. These data directly demonstrate attenuated binding of fXa**R347N** to fVa on a phospholipid surface in the absence of prothrombin.

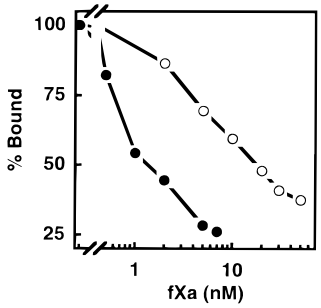

FIGURE 6: Competition binding assay. PC:PS coated latex beads (0.2%, v/v) were incubated for 10 min in the presence fVa (1 nM). [^{125}I]fXa**S379** (1nM) was added with various concentrations of unlabeled fXa**WT** [0−7 nM (●)] or fXa**R347N** [0−50 nM (○)] and incubated for an additional 10 min. The beads were collected by centrifugation and counted. The amount of specific binding (fVa, phosphatidylserine, and calcium dependent) was determined and expressed as the percent of binding in the absence of unlabeled fXa. Nonspecific binding (fVa-independent) was subtracted from all reactions.

DISCUSSION

We have characterized a recombinant fX with asparagine substituted for arginine at position 347. The mutation has no discernible impact on synthesis or secretion in our expression system. Moreover, normal activation of fX**R347N** by fVIIa/TF, fIXa/fVIIIa and RVV-X, and normal interaction of fXa**R347N** with Spectrozyme FXa, prothrombin, ATIII, and TFPI attest to normal folding and active-site geometry.

Arg347 is part of a large basic epitope that Padmanabhan and co-workers have described as a heparin-binding domain (*23*). The loss of the charge contributed by this residue likely weakens the fXa−heparin interaction, thereby causing the reduced (~6-fold) impact of heparin on the inhibition of fXa**R347N** by ATIII. Acceleration of inhibition by the pentasaccharide, which need only interact with ATIII to have its effect, is normal. To ensure sensitivity of rate constant determinations to the mutation, the concentrations of pentasaccharide and heparin tested were empirically determined to support half-maximal acceleration of inhibition of fXa**WT**. Rigorous analysis of the contribution of Arg347 to heparin binding and functional definition of the complete heparin-binding domain will require additional mutagenesis studies.

In addition to the effect on heparin binding, we find that Arg347 is important for the interaction between fXa and fVa. In the absence of phospholipid, fVa had no effect on prothrombin activation by fXa**R347N** at concentrations that enhanced fXa**WT** catalysis by 3 orders of magnitude. Since fVa enhances the catalytic activity of fXa by mediating conformational changes in the enzyme (*25*, *26*), we considered the possibility that Arg347 could somehow be required for those rearrangements, but not for fVa binding. However, if a crucial rearrangement were blocked by the substitution,

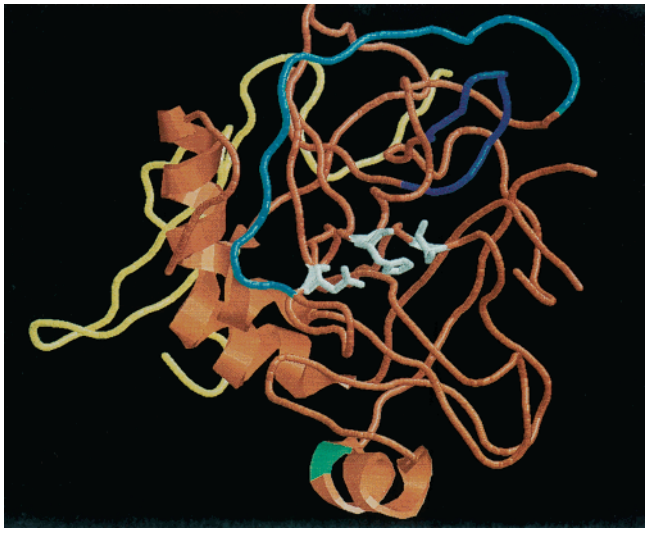

FIGURE 7: Model of fXa and Arg347. The image of fXa was generated using RasMol v2.5. In the illustration, the serine protease domain is orange, EGF-1 is yellow, and the surface loops identified by Chattopadhyay et al. as fVa binding epitopes are depicted in dark and light blue (*35*). The catalytic triad is represented in white and the position of Arg347 is highlighted in green.

the fVa-accelerated rate of thrombin generation by fXa**R347N** would likely be reduced even when all complex components had been optimized. Contrary to this, given the physiological phospholipid surface and excess fVa of activated platelets, fXa**WT** and fXa**R347N** have equivalent catalytic potential. Moreover, a competitive binding assay directly demonstrated a reduced affinity of fXa**R347N** for fVa on a phospholipid surface. Since this assay does not contain prothrombin, the results reflect the association of fXa with fVa rather than a potential fVa/prothrombin complex.

Due to limited availability of human fVa, bovine fVa is commonly employed for determination of the affinity between fVa and fXa (*11*, *33*−*34*). The use of human fVa in this study precluded the use of saturating concentrations of cofactor in thrombin formation assays with fXa**R347N** on PC:PS vesicles. However, the affinity of fXa**R347N** for fVa was at least 5-fold lower than that of fXa**WT** under these conditions. If the enzymes have equivalent maximum turnover rates, as indicated by the results with activated platelets, the calculated apparent affinity of fXa**R347N** for fVa on PC:PS vesicles is ∼20-fold lower than the cofactor affinity of fXa**WT.** Regardless of the maximum turnover rate, fXa**R347N** clearly demonstrates a significantly reduced affinity for fVa on a PC:PS surface.

Chattopadhyay et al., based on the inhibition of functional assays by peptides mimicking linear sequences of fX, concluded that residues 211−222 and 254−274 in fXa are important for interactions with fVa (*35*). These sequences are shown in dark and light blue in Figure 7, an illustration of the fXa structure reported by Padmanabhan and co-workers (*23*). They are some distance from Arg347, whose position is shown in green. Although it is possible that substitution of Arg347 attenuates fVa binding by somehow perturbing the structure of a distant binding epitope (e.g., residues 211−222 and 254−274), we believe it is more likely that Arg347 actually is part of the fVa binding site of fXa. First, based on examination of the fXa crystal structure, there is no obvious scenario in which changing Arg347 to asparagine could cause a rearrangement apparent across the molecule without having any impact on activation, catalysis or inhibition. Second, the sequence of fVIIa corresponding to residues 346−349 in fX (164−167 in chymotrypsin numbering), together with regions of its EGF2 domain, forms a contact surface with TF based on the recently solved fVIIa/TF crystal structure (*36*). The homologous residues in fX might well interact with fVa. Finally, fXa bound to fVa is protected from inhibition by antithrombin III and heparin (*37*). It is appealing to hypothesize that part of this protection is a consequence of the overlap of heparin- and fVa-binding sites on fXa. Just as is the case for fVIIa and TF, it is likely that many other residues besides Arg347 are important for fXa interaction with fVa. Definition of the entire surface contact will require additional mutagenesis studies or a crystal structure of the complex.

This substitution also creates a potential, though unused, site for N-linked glycosylation. Protein C is usually glycosylated (*38*−*40*) at Asn329 (PVVPHNECS), although it is unusual in that cysteine rather than the typical serine or threonine follows two residues after the modified asparagine. In contrast, fX is not glycosylated at the homologous residue, Asn348 (PYVDRNSCK). In fact, all N-linked carbohydrate on fX is attached to the peptide released on activation, residues 143−194. Introduction of the typical glycosylation site in fX**R347** juxtaposed with the atypical site (PYVD-**N**NSCK) still did not result in glycosylation in this region. We propose that this region of fX is "protected" from glycosylation such that Asn348 is not modified and the integrity of the factor Va-binding site is not compromised. It may be that this sequence is less accessible in fX than in protein C because some structural element unique to fX masks the region. The activation peptide is an attractive candidate. With several carbohydrate side chains and 40 more amino acids than the activation peptide of protein C, it could easily "cover" Asn348 and the surrounding residues. Upon release of the peptide by activation, the site would become accessible for interaction with fVa. This, in turn, might explain why zymogen fX is ineffective in competing with fXa for fVa binding (*41*).

ACKNOWLEDGMENT

We would like to thank Tom Girard and Kevin Conricode for their critical review of the manuscript.

REFERENCES

1. Jesty, J., Spencer, A. K., and Nemerson, Y. (1974) *J. Biol. Chem. 249*, 5614−5622.
2. DiScipio, R. G., Hermodson, M. A., and Davie, E. W. (1977) *Biochemistry 16*, 5253−5260.
3. Pfeiffer, R. A., Ott, R., Gilgenkrantz, S., and Alexandre, P. (1982) *Hum. Genet. 62*, 358−360.
4. Nemerson, Y., and Bach, R. (1982) *Prog. Hemostasis Thromb. 6*, 237−261.
5. Nemerson, Y. (1986) *Blood 71*, 1−8.
6. Mann, K. G., Jenny, R. J., and Krishnaswamy, S. (1988) *Annu. Rev. Biochemistry 57*, 915−956.
7. Rosenberg, R. D., and Damus, P. S. (1973) *J. Biol. Chem. 248*, 6490−6505.
8. Owen, B. A., and Owen, W. G. (1990) *Biochemistry 29*, 9412−9417.
9. Broze, G. J., Jr., Warren, L. A., and Novotny, W. F., et al. (1988) *Blood 71*, 335−343.

10. Girard, T. J., Warren, L. A., Novotny, W. F., Higuchi, D. A., Girard, J. J., and Miletich, J. P. (1989) *Nature 338*, 518−520.
11. Krishnaswamy, S. (1990) *J. Biol. Chem. 265*, 3708−3718.
12. Rudolph, A. E., Mullane, M. P., Porche-Sorbet, R. P., Tsuda, T., and Miletich, J. P. (1996) *J. Biol. Chem. 271*, 28601−28606.
13. Rudolph, A. E., Mullane, M. P., Porche-Sorbet, R. P., Tsuda, T., and Miletich, J. P. (1997) *Protein Expression Purif. 10*, 373−378.
14. Broze, G. J., Jr., and Miletich, J. P. (1984) *J. Clin. Invest. 73*, 933−938.
15. Fass, D. N., Knutson, G. J., and Katzmann, J. A. (1982) *Blood 59*, 594−600.
16. Kisiel, W., Hermodson, M. A., and Davie, E. W. (1976) *Biochemistry 15*, 4901−4906.
17. Laemmli, U. K. (1970) *Nature 227*, 680−685.
18. MacDonald, R. C., MacDonald, R. I., Menco, B. Ph. M., Takeshita, K., Subbarao, N. K., and Hu, L. (1991) *Biochim. Biophys. Acta 1061*, 297−303.
19. Graham, F. L., and Eb, A. J. (1973) *Virology 52*, 456−467.
20. Huang, Z., Wun, T., Broze, G. J., Jr. (1993) *J. Biol. Chem. 268*, 26950−26955.
21. Olson, S. T., Bjork, I., and Shore, J. D. (1993) *Methods Enzymol. 222*, 525−559.
22. Kalafatis, M., Xue, J., Lawler, C. M., and Mann, K. G. (1994) Biochemistry *33*, 6538−6545.
23. Padmanabhan, K., Padmanabhan, K. P., Tulinsky, A., Park, C. H., Bode, W., Huber, R., Blankenship, D. T., Cardin, A. D., and Kisiel, W. (1993) *J. Mol. Biol. 232*, 947−966.
24. Craig, P. A., Olson, S. T., and Shore, J. D. (1989) *J. Biol. Chem. 264*, 5452−5461.
25. Husten, J. E., Esmon, C. T., and Johnson, A. E. (1987) *J. Biol. Chem. 262*, 12953−12961.
26. Walker, R. K., and Krishnaswamy, S. (1993) *J. Biol. Chem. 268*, 13920−13929.
27. Dahlback, B., and Stenflo, J. (1978) *Biochemistry 17*, 4938−4945.
28. Tracy, P. B., Nesheim, M. E., and Mann, K. G. (1981) *J. Biol. Chem. 256*, 743−751.
29. Rosing, J., Tans, G., Grovers-Riemslag, J. W., Zwaal, R. F., and Hemker, C. (1980) *J. Biol. Chem. 255*, 274−283.
30. Nesheim, M. E., Tracy, R. P., and Mann, K. G. (1984) *J. Biol. Chem. 259*, 1447−1453.
31. Boskovic, D. S., Giles, A. R., and Nesheim, M. E. (1990) *J. Biol. Chem. 265*, 10497−10505.
32. Pryzdial, E. C. G., and Mann, K. G. (1991) *J. Biol. Chem. 266*, 8969−8977.
33. Nesheim, M. E., Taswell, J. B., and Mann, K. G. (1979) *J. Biol. Chem. 254*, 10952−10962.
34. Nesheim, M. E., Kettner, C., Shaw, E., and Mann, K. G. (1981) *J. Biol. Chem. 256*, 6537−6540.
35. Chattopadhyay, A., James, H. L., and Fair, D. S. (1992) *J. Biol. Chem. 267*, 12323−12329.
36. Banner, D. W., D'Arcy, A., Chene, C., Winkler, F. K., Guha, A., Konigsberg, W. H., Nemerson, Y., and Kirchhofer, D. (1996) *Nature 380*, 41−46.
37. Lindhout, T., Baruch, D., Schoen, P., Franssen, J., and Hemker, C. (1986) *Biochemistry 25*, 5962−5969.
38. Stenflo, J., and Fernlund, P. (1982) *J. Biol. Chem. 257*, 12180−12190.
39. Miletich, J. P., and Broze, G. J., Jr. (1990) *J. Biol. Chem. 265*, 11397−11404.
40. Grinnell, B. W., Walls, J. D., and Gerlitz, B. (1991) *J. Biol. Chem. 266*, 9778−9785.
41. Miletich, J. P., Jackson C. M., and Majerus P. W. (1978) *J. Biol. Chem. 253*, 6908−6916.

BI992379B